Activation of energy metabolism through growth media reformulation enables a 24-hour workflow for cell-free expression

Max Z. Levine[1,3], Byungcheol So[2,3], Alissa C. Mullin[2,3], Rob Fanter[4], Kayla Dillard[,5], Katharine R. Watts[2,3], Michael R. La Frano[5,6*], Javin P. Oza[2,3,*]

[1]Department of Biological Sciences, California Polytechnic State University, San Luis Obispo, CA, 93407, USA

[2]Department of Chemistry and Biochemistry, California Polytechnic State University, San Luis Obispo, CA, 93407, USA

[3]Center for Application in Biotechnology, California Polytechnic State University, San Luis Obispo, CA, 93407, USA

[4]College of Agriculture, Food and Environmental Sciences, California Polytechnic State University, San Luis Obispo, CA, 93407, USA

[5]Department of Food Science and Nutrition, California Polytechnic State University, San Luis Obispo, CA, 93407, USA

[6]Center for Health Research, California Polytechnic State University, San Luis Obispo, CA, 93407, USA

KEYWORDS cell-free protein synthesis, synthetic biology, metabolomics, in vitro transcription/translation, autoinduction

ABSTRACT: Cell-free protein synthesis (CFPS) platforms have undergone numerous workflow improvements to enable diverse applications in research, biomanufacturing, and education. The *Escherichia coli* cell extract-based platform has been broadly adopted due to its affordability and versatility. The upstream processing of cells to generate crude cell lysate remains time-intensive and technically nuanced, representing one of the largest sources of cost associated with the biotechnology. To overcome these limitations, we have improved the processes by developing a long-lasting autoinduction media formulation for CFPS that obviates human intervention between inoculation and harvest. The cell-free autoinduction (CFAI) media supports the production of robust cell extracts from high cell density cultures nearing stationary phase of growth. As a result, the total mass of cells and the resulting extract volume obtained increases by 400% while maintaining robust reaction yields of reporter protein, sfGFP (>1 mg/ml). Notably, the CFAI workflow allows users to go from cells on a streak plate to completing CFPS reactions within 24 hours. The CFAI workflow uniquely enabled us to elucidate the metabolic limits in CFPS associated with cells grown to stationary phase in the traditional 2x YTPG media. Metabolomics analysis demonstrates that CFAI-based extracts overcome these limits due to improved energy metabolism and redox balance. Advances reported here shed new light on the metabolism associated with highly-active CFPS reactions, and inform future efforts to tune the metabolism in CFPS systems. Additionally, we anticipate that the improvements in the time and cost-efficiency of CFPS will increase the simplicity and reproducibility, reducing the barriers for new researchers interested in implementing CFPS.

Cell-free protein synthesis (CFPS) platforms have provided a robust, flexible, and accessible strategy to express high titers of proteins for the scientific community.[1] The open nature of the platform enables researchers to monitor protein expression in real time, to alter reaction conditions, and to produce traditionally intractable proteins on-demand. CFPS systems have undergone numerous and significant developments over the last 50 years, resulting in long-lived reactions with improved yields at lower costs.[2] The *Escherichia coli*-based CFPS platform in particular has gained traction over the last 30 years and has surpassed the Wheat Germ and Rabbit Reticulocyte platforms in cumulative publications.[1] The broad adoption of the *E. coli*-based crude extracts for CFPS is in part a function of consistent effort by the scientific community to enhance robustness of the platform, streamline the workflow of generating and utilizing cell extracts, and expand the utility and accessibility for new users. From its inception in the 1950s when Nirenberg and Matthaei first used CFPS to decipher the genetic code, there have been numerous advances in both energy systems and laboratory workflows to make CFPS a viable protein expression platform for applications ranging from discovery through manufacturing.[3] Energy systems have been consistently tuned to allow for high protein titers while regenerating substrates to allow for longer lasting reactions with reduced costs.[4] Workflows for cell growth, lysis, and extract prep have also undergone optimizations. Examples include, but are not limited to: growth within baffled flasks[5–8], the advancement of sonication-based lysis[5,6,8] or bead beating[8,9], the utilization of tabletop centrifuges to separate transcriptional and translational machinery from cell lysate[5–9], and the ability to perform extract preparation at the 100 L-scale.[10] Most of these advances improved the downstream processing, from cell lysis to CFPS reaction conditions, leading to long-lived, high-yielding reactions that are also capable of producing traditionally intractable proteins. The primary improvement to upstream processing over the last 15 years has been the increasing use of baffled shake flasks for cell growth instead of fermenters; otherwise, the process of growing and harvesting cells appears to have remained unchanged.[5,11]

The upstream processing involved in generating *E. coli*-based crude extracts represents a laborious and technically nuanced process that can contribute to variability within CFPS reactions between laboratories and users alike.[12,13] In fact, the development of best practices for cell lysate preparation is one of six key recommendations emerging from the National Institutes of Standards and Technology workshop on cell-free.[13] This recommendation is an outcome of the working group's assessment that cell extract preparation remains non-standardized, expensive, and irreproducible. In order to overcome these limitations, we sought to shorten and simplify the workflow and lower the barrier-to-entry for implementing CFPS by limiting the researcher oversight required in the extract preparation process. This goal was identified based on the observations that the researcher is often the primary source of both variability in extract preparation, as well as the cost.

Here we define upstream processing as the steps involved in the cell growth and harvesting, starting from the originating cell colonies through cell lysis for crude extract preparation. The impetus for improving this workflow is two-fold: A) to reduce the number of technical steps as well as the time and labor associated with upstream processing and B) to improve reproducibility of CFPS from batch-to-batch, user-to-user, and across institutions.[5,6,8,9,11,13] The existing upstream workflow represents the most time-consuming aspect of cell-free protein synthesis, requiring up to 2 days of researcher labor to generate cell extract.[9,12] This workflow entails 1) growing a seed culture overnight from an existing, viable streak plate made from a glycerol stock; 2) inoculate large volume growths with OD600 monitoring for induction of T7 RNAP and harvest at precise phases of growth; 3) perform multiple bacterial pellet washing resuspensions prior to storage of cell pellets for later lysis.[5–7,11] Downstream processing steps of cell lysis and CFPS reactions can be done immediately following harvest, but often follows on a third day of labor that may occur much later in time.

Toward our goal, we have developed a cell-free autoinduction (CFAI) media formulation (Supplemental Table 1) for *E. coli* BL21Star™(DE3) that enables researchers to obviate the most nuanced and burdensome steps of the existing upstream processing workflow. The outcome is the simplification of a 3-day workflow down to a 24-hour workflow (Figure 1) that can be implemented in a 'set-it and forget-it' manner. Notably, CFAI supports cell growth to high cell densities without sacrificing cell extract productivity. The result is a >400% increase in cell mass obtained and a corresponding >400% increase in total extract volume obtained. Our new approach is simple, reproducible, and decreases the time and labor required, while also increasing the quantity of robust cell extract obtained. Together, the advantages will further reduce the barrier to broad adoption of the CFPS platform.

The capacity to generate robust cell extracts from stationary phase cultures is a key advance toward supporting the 24-hour workflow. Prior work has suggested that harvesting cells at early-to-mid log phase of growth is ideal as both the quantity and quality of translation machinery is increased to support cells that are actively doubling.[5,14–17] Given that the CFAI extracts from stationary phase did not show any functional limits in protein synthesis, we hypothesized that conditions of cell growth and harvest affect the metabolism in cell-free systems. We therefore pursued metabolomics analysis to understand the basis for achieving highly active cell extracts mediated by the CFAI method. We report novel insights into the metabolic features associated with both inactive and active cell extracts generated from cells harvested at both mid-log and stationary phases of growth. This work provides an improved workflow

for generating robust extracts, and the development of this workflow has shed light into the metabolism of cell-free systems that can be leveraged more broadly.

Results

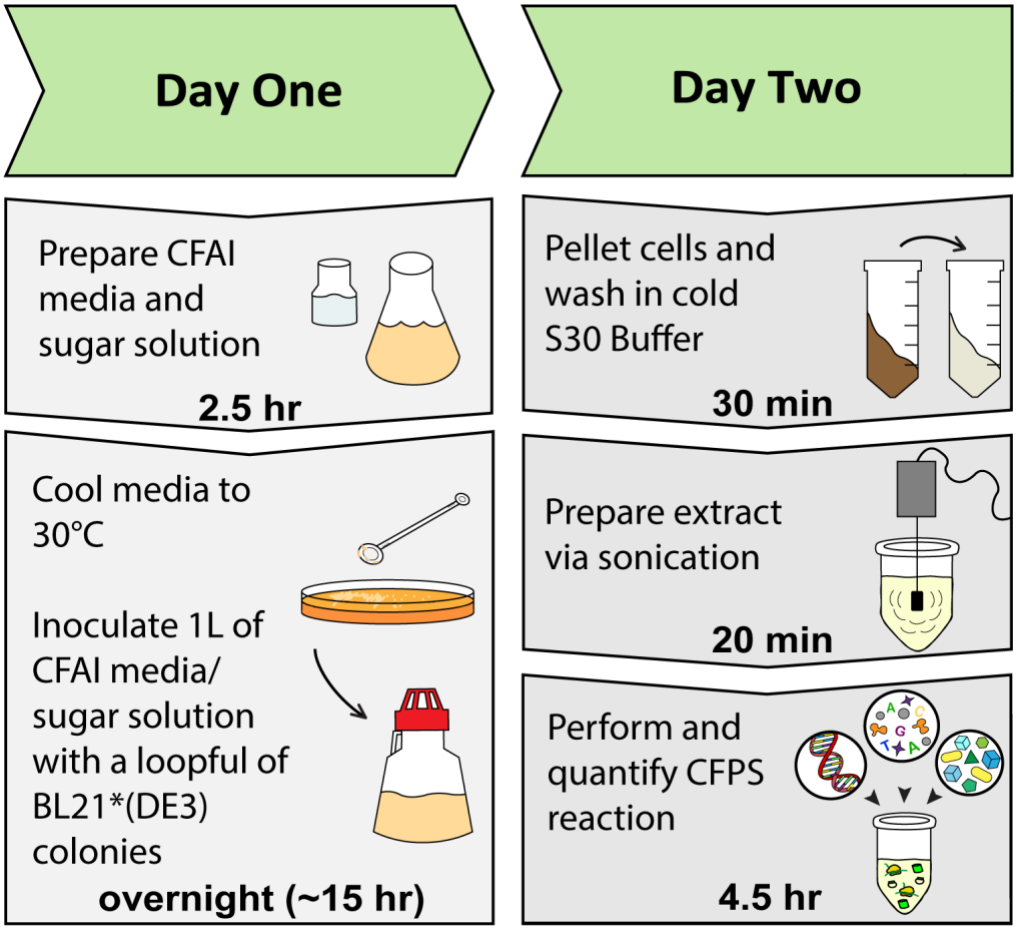

Figure 1. Schematic and timeline the CFAI workflow.

Upstream Processing

In efforts to reduce the time and labor associated with obtaining cells for extract preparations, we first assessed whether three wash cycles of the bacterial pellet were necessary prior to lysis of the cells. We determined that performing one wash instead of three is not detrimental to the resulting cell extracts' capacity to express the reporter protein sfGFP (Supplemental Figure 1).[5,8] From this point onward, each cell pellet underwent only one wash regardless of media type. Additionally, we did not perform a runoff reaction as it is not necessary for the BL21Star™(DE3) strain.[5]

Next, an autoinduction strategy was employed to obviate the need to induce cells with IPTG, the lactose analog. An autoinduction media recipe adopted from F.W. Studier[18] is similar to 2x YTPG in quantities of yeast extract, tryptone, and phosphate salts, but differs significantly in carbon sources, significantly reducing the amount of glucose in favor of added lactose and glycerol (Supplemental Table 1). Replacement of glucose with lactose and glycerol as carbon sources was of concern given that glucose (G) supplementation in 2x YTP was first developed to limit the expression of alkaline and hexose phosphatases that would normally result in a buildup of inorganic phosphates, metabolites detrimental

to the CFPS reaction as well as to activate central metabolism for energy recycling within the CFPS reactions.[14,19] To our surprise, replacing 2x YTPG with autoinduction media did not negatively affect the extract's capacity to perform *in vitro* transcription and translation when cells were harvested at an OD_{600} of 2.5 (Figure 2). Autoinduction obviates the need to monitor OD_{600} for T7 RNAP induction, when combined with performing 1 wash instead of 3 washes during harvest, we observed noteworthy improvements to the overall workflow (Supplemental Figure 1). However, growth in autoinduction media remains dependent on harvesting cells within a precise window of cell growth- during the early to mid-log phase at which point cells are undergoing rapid doubling and ribosomes and associated translational proteins are thought to be in high abundance.[5,15–17] A downside to this approach is that it tethers the researcher to monitoring cell densities for the duration of the growth, increasing the labor and variability

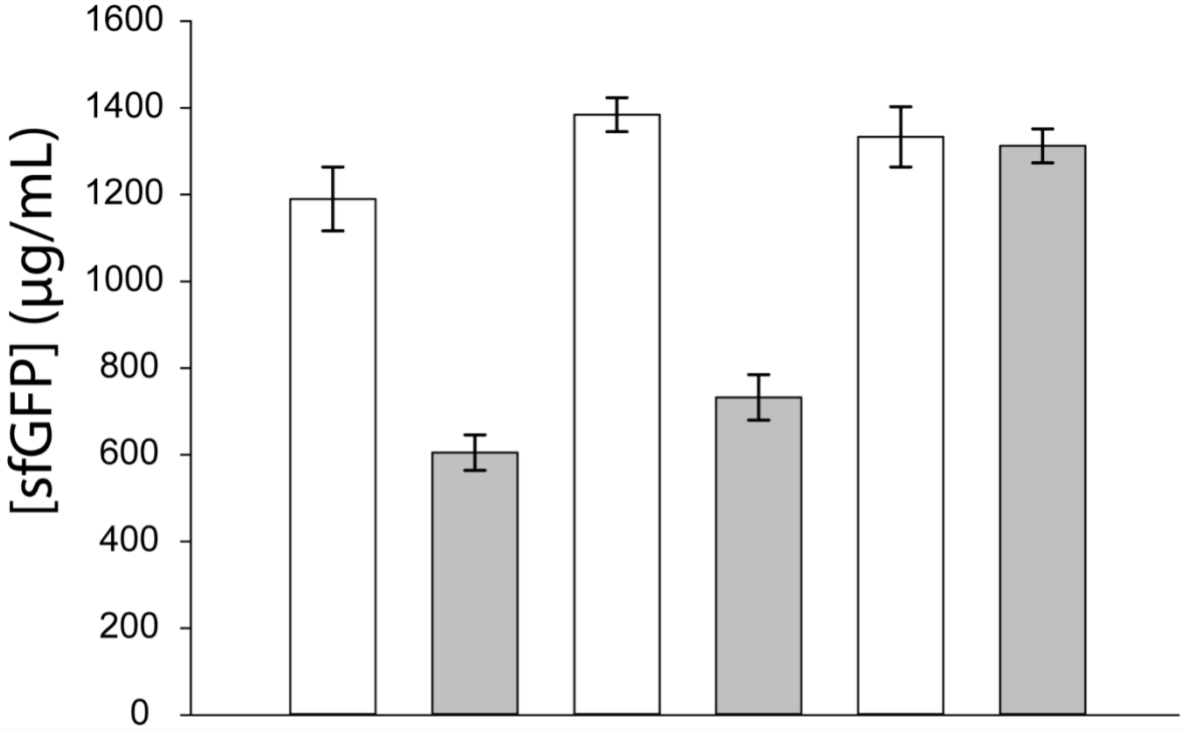

Media	2xYTPG		Autoinduction		**CFAI**	
OD_{600} at Harvest	2.5	10	2.5	10	2.5	10
Origin	Kim, R.G. & Choi, Y.C., 2000		Studier, 2005		**This Work**	

Figure 2. CFAI media recipe enables robust extract when harvested at an OD_{600} of 10. All values are based upon triplicate measurements from three independent growths, three independent extract preparations, and three independent CFPS reactions across all media types. Error bars represent one standard deviation of the average of three independent reactions for each condition performed in triplicate. Bolded ingredients represent modifications from the 2x YTPG media formulation.

associated with obtaining cells for CFPS.[12] We sought to re-evaluate the previous observations that

established the optimal OD_{600} for harvesting cells.[5,7] Toward this end, cells were grown to high densities, OD_{600} of 10, in both 2x YTPG and autoinduction media. Our observations confirmed previous findings that extracts generated from cells harvested at the stationary phase of growth in either 2x YTPG or autoinduction media show a depressed capacity for protein production compared to extracts generated from cells harvested at an OD_{600} of 2.5 (Figure 2).

Table 1. **Cell pellet mass and extract volume generated from corresponding media types grown in triplicate. Values were averaged across triplicate growths.**

	2x YTPG		AI		CFAI	
OD_{600}	2.5	10	2.5	10	2.5	10
pH at Harvest	7.0	5.4	7.0	6.3	7.1	6.7
Cell Pellet (g)	4.21	14.22	4.79	17.4	4.13	13.9
Extract Volume (mL)	4.29	17.16	5.13	20.52	4.41	17.64

We then sought to identify whether the necessity to harvest cells at mid-log phase of growth is a result of functional limitations other than translation machinery. We observed that depressed CFPS yields from high cell density cultures correlate with more acidic culture conditions at harvest (Table 1). To test the role of pH destabilization, we increased the buffering capacity of the AI media by two-fold. Additionally, we hypothesized that the extended growth times may exhaust the lactose carbon source available in the AI media, resulting in depressed expression of T7 RNAP and/or altered metabolism of the cells, becoming incompatible with the PANOxSP energy system in our CFPS reactions. To address these concerns, we also increased the lactose concentration by two-fold within the AI media (Supplemental Table 1). Cells grown in the modified AI media formulation were first cultured to an OD_{600} of 2.5 in order to establish whether the added buffering capacity and lactose can support cell growth for obtaining robust extracts. Indeed, extract resulting from the modified AI media reproducible yielded >1 mg/mL of reporter protein sfGFP (Figure. 2). Cells were then grown to an OD_{600} of 10 in the modified AI media, washed once, and processed for extract preparation. The extract resulting from cells grown to high densities also resulted in highly active cell extracts capable of producing >1 mg/mL of reporter protein sfGFP (Figure 2). We considered the possibility that the improved buffering capacity alone may be responsible for the benefits observed with CFAI media. Doubling the buffering capacity of 2x YTPG to match that of CFAI improved yields of extracts from OD_{600} 10 harvests from 605 ± 41 µg/ml to 744 ± 69 µg/ml, but remained insufficient to rescue the full productivity of the 2x YTPG extract prepared from OD_{600} 2.5 harvests (1192 ± 80 µg/ml). These findings demonstrated that our cell-free autoinduction (CFAI) media formulation overcomes and expands the limits of the traditional cell growth workflow.

In order to maximize the potential of CFAI media, we further evaluated the optimal concentration of each component of the media formulation. Toward this end, we tuned the carbon source concentrations, and timings of carbon source supplementation. Increased concentrations of glycerol were added to the sugar recipe but provided no boost to the overall cell density or extract productivity (Supplemental Figure 2). To test the hypothesis that metabolic shifts as cells approach stationary phase

play a role in limiting extract productivity, we also tested growth conditions in which glycerol was spiked into high density cultures 1 hour prior to harvest in efforts to reactivate metabolism. These interventions also did not improve overall cell density or extract productivity compared to CFAI media. Efforts to tune the CFAI media formulation confirmed that the optimal conditions require minimal human intervention in the workflow. We chose to maintain the concentration of glucose in AI media in order to provide the adequate threshold of energy in the media to begin expressing the enzymes needed to uptake and begin metabolizing lactose.[18,20]

To identify whether the full potential of CFAI was limited in other resources, yeast extract and tryptone were also augmented based on the SuperBroth media recipe that is marketed for high density cultivation of *E. coli* cells.[21] The resulting Super-CFAI media displayed similar OD_{600} values and extract productivity levels as the CFAI media. These findings suggest that the added cost of reagents for the Super-CFAI media are not justified and that the CFAI media formulation is optimal (Supplemental Figure 3).

The capacity to obtain highly productive cell extracts from high density cell cultures using CFAI media liberates the researcher from the time and labor associated with existing workflows for cell growth. To expand on this capacity, we sought to reduce or remove human intervention from all cell growth steps involved in the upstream processing. Specifically, the traditional workflow requires the researcher to 1) inoculate “over-night” seed cultures from a single colony grown on a recent, viable streak plate, 2) inoculate larger volumes of media with the seed culture, and 3) monitor growth of cells that will ultimately generate cell extract capable of robust *in vitro* transcription and translation. Given the slow nature of cell propagation, this process consumes 2 days. We therefore tested a modified inoculation workflow in which multiple colonies (Supplemental Figure 4) of BL21Star™(DE3) from a viable streak plate were inoculated directly into 1 L of CFAI media, incubated for 15 hours overnight, and harvested the subsequent morning. This experiment was conducted at both 30°C and 37°C, and the resulting OD_{600} values were 8.0 and 10.0 respectively, generating cell pellets of 15 g and 18 g respectively. Cells were washed once during harvest and lysed via sonication for extract preparation. Extracts from both overnight growths were robust, yielding >1 mg/mL of sfGFP, with the 30°C growth producing a ~10% higher titer than the 37°C growth. If viable streak plates and CFAI media are available, this new workflow enables researchers to inoculate a liquid culture at 5 p.m., harvest at 8 a.m., generate extracts by 10 a.m., setup CFPS reactions by noon, and quantify by 3-4 p.m. In other words, this new CFAI-based workflow enables researchers to go from cell colonies on a streak plate to conducting and analyzing CFPS within 24 hours. Notably, this workflow requires less than 6 hours of a researcher’s active effort.

CFAI-based high density cell growth provides advantages beyond improved workflows. The quantity of cells obtained from high density growths are ~4 times greater, and the corresponding extract volumes obtained are also ~4 times larger (Table 1). As a function of the simplicity, the CFAI-based workflow is also highly reproducible. To evaluate this, we grew three independent cultures of each condition, performed three independent extract preparations of each growth, tested each extract in triplicate CFPS reactions, and subsequently quantified productivity of each reaction in triplicate. The standard deviation resulting from these independent replicates is under 10% (Figure 2) underscoring the reproducibility of the approach. Having shared the CFAI workflow through biorxiv.org in the August of 2019, we have received positive feedback from researchers within the broader cell-free community about the utility and reproducibility of this workflow as described. Lastly, while the cost of 2x YTPG and CFAI media components are similar, the removal of the need for IPTG, combined with reduced researcher time and the overall increase in extract volume produced, makes this new approach significantly more cost-effective.

Metabolomics analyses

Development of the CFAI workflow uniquely enabled us to evaluate the metabolic basis for poor-quality extracts as well as highly-productive extracts in a growth phase dependent manner. Metabolomics analysis was performed on cell extracts generated from cells harvested at OD_{600} 2.5 and OD_{600} 10 grown in the traditional media 2x YTPG, as well as AI and CFAI media. In addition to the analysis of cell extracts, metabolomics analysis was also performed once CFPS reactions were completed (post-reaction) using extracts from varying growth ODs and growth media formulations. While the metabolome of the cell extracts is insightful, the metabolome of the post-reaction samples provided valuable insights into the active metabolism that is present in cell extracts, and we demonstrate that this is growth medium dependent.

Through a combination of various growth media, differing harvest OD_{600}, and extract vs. post reaction samples, 12 unique conditions for metabolomics analysis are represented in this study. A total of 88 metabolites were detected in both the extract and post-reaction samples (Supplemental Metabolomics Data). Principal Component Analysis (PCA) of the extract samples discriminated the CFAI OD_{600} 10 and AI OD_{600} 10 groups along component 1 from all other groups. 2x YTPG OD_{600} 10 extracts showed separation along component 2 (Figure 3). PCA of the post-reaction samples discriminated all OD_{600} 10 samples from OD_{600} 2.5 samples along component 3 (Figure 3). For the post-reaction samples,

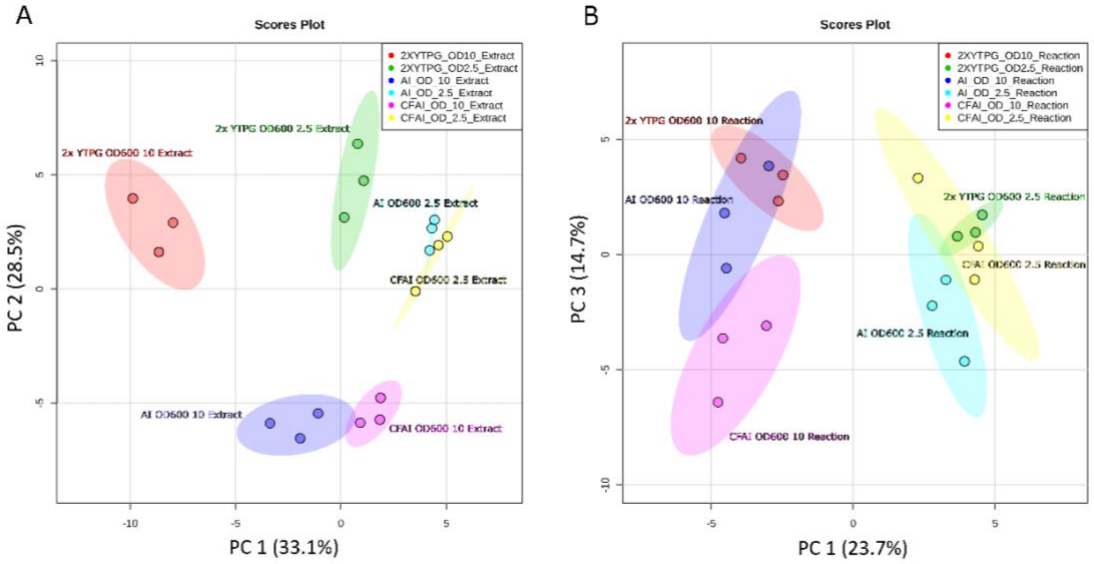

Figure 3. PCA analysis to visualize group discrimination in a 2-dimensional scores plot showed a separation of sample groups. Each point represents an individual replicate and color of point denotes the experimental condition. The extract samples (A) projected from their group centroid along components 1 and 2 showed a separation between the AI OD_{600} = 10 and CFAI OD_{600} = 10 experimental groups along component 1 while the reaction samples (B) projected from their group centroid along components 1 and 3 showed a separation between the OD_{600} = 2.5 and OD_{600} = 10 experimental groups along component 3. Separation existed between CFAI OD_{600} = 10 and the other OD_{600} = 10 groups along component 1.

there was separation between CFAI OD_{600} 10 and the other OD_{600} 10 groups along component 1 (Figure 3). PCA of extract and post-reaction samples demonstrate that the metabolome resulting from cells grown in CFAI to OD_{600} 10 is distinct from all other samples (Figure 3).

For the cell extracts, univariate analysis identified 60 metabolites that were significantly different between groups ($p<0.05$), including 58 that passed false discovery rate (FDR) (FDR<0.05) (Supplemental Metabolomics Data). A particular focus of this experiment was to differentiate the metabolomic profile of CFAI OD_{600} 10 versus other OD_{600} 10 extracts from cells grown in 2x YTPG and AI media, harvested at OD_{600} of 2.5 or 10. Among the cell extract samples, alpha-hydroxybutyrate concentration was significantly higher in the CFAI OD_{600} 10 group than the other groups (Supplemental Metabolomics Data). Increased production of alpha-hydroxybutyrate has been linked to the presence of a high NADH + H^+/NAD^+ ratio and glutathione anabolism.[23] Tryptophan and several of the intermediates in the tryptophan conversion to niacin pathway were altered as well (Figure 4). Tryptophan concentrations were higher in CFAI and AI OD_{600} 10 extracts than 2x YTPG OD_{600} 10 (Figure 4). Kynurenic acid and xanthurenic acid concentrations were higher in CFAI OD_{600} 10 versus 2x YTPG OD_{600} 10 and showed a trend elevation versus AI OD_{600} 10 ($p=0.1$) (Figure 4). Concentrations of niacinamide and quinolinic acid, NAD precursor and/or breakdown products, in CFAI OD_{600} 10 extracts were higher than AI harvested at

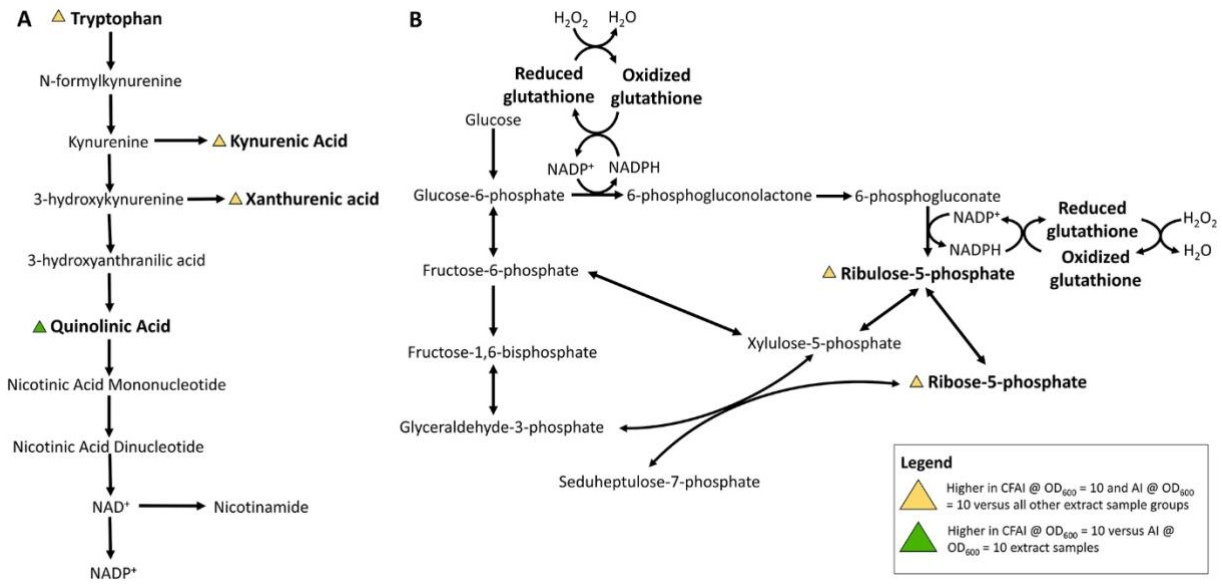

Figure 4. Altered metabolic pathways identified in *E. coli*-based cell extracts. Specific metabolites with altered abundance identified in the metabolomics analysis are bolded. Colored shapes indicate the specific condition in which a metabolite's abundance is altered. Metabolic pathways altered included the tryptophan-niacin conversion pathway (A) and pentose phosphate pathway (B).

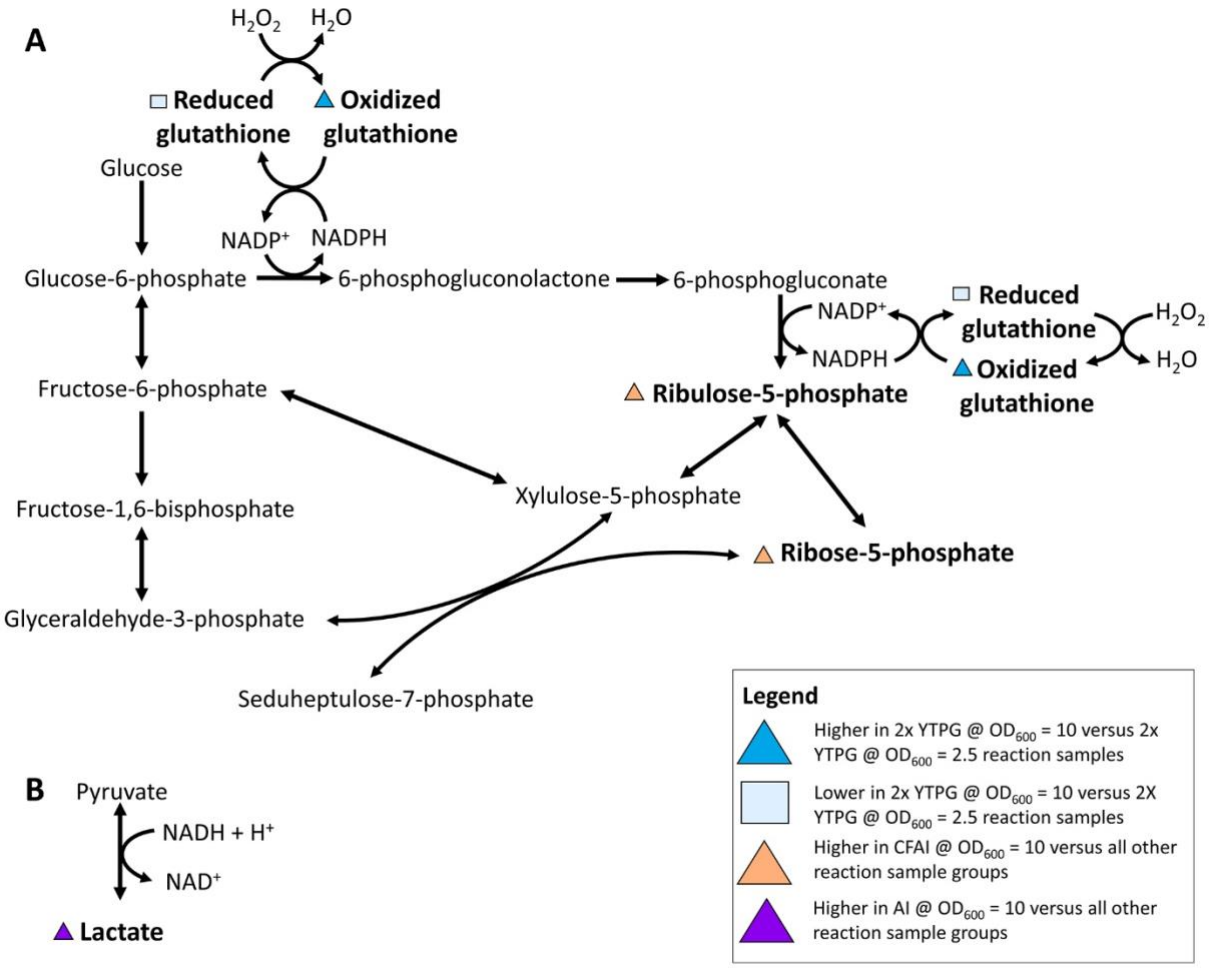

Figure 5. Altered metabolic pathways identified upon completion of CFPS reactions. Specific metabolites with altered abundance identified in the metabolomics analysis are bolded. Colored shapes indicate the specific content in which a metabolite's abundance is altered. Metabolic pathways altered included the pentose phosphate pathway (A) and the pyruvate-lactate pathway (B). "Reaction samples" label corresponds to samples collected and analyzed post-CFPS reactions.

OD_{600} 10 (P=0.05) (Figure 4).[2425]. Concentrations of the pentose phosphate pathway metabolites SUM_ribose-5-phosphate/ribulose-5-phosphate in CFAI and AI OD_{600} 10 extracts were higher than 2x YTPG OD_{600} 10 (Figure 4). Overall, the cell extract metabolomes for AI OD_{600} 10 and CFAI OD_{600} 10 were similar to each other, with the exception of quinolinic acid and nicotinamide levels, but notably distinct from 2x YTPG OD_{600} 10 (Supplemental Metabolomics Data). While these observations are consistent with the similarity in the AI and CFAI media formulations, their metabolomes do not clearly explain why CFAI OD_{600} 10 extracts are more productive than AI OD 10 extracts.

In addition to evaluating cell extracts, we also performed metabolomics analysis on the post-reaction milieu. Amongst the post-reaction samples, univariate analysis identified 38 metabolites that were significantly different between groups ($p<0.05$), including 31 that passed FDR (FDR<0.05) (Supplemental Metabolomics Data). Focusing on the difference between CFAI OD_{600} 10 versus the other OD_{600} 10

groups, CFAI OD_{600} 10 post-reaction samples had lower concentrations of 2-hydroxyglutarate compared to the other conditions, perhaps reflecting a relatively lower NADH + H^+/NAD^+ ratio and a non-acidic pH (Supplemental Metabolomics Data).[26] Tryptophan conversion to niacin pathway metabolites were altered including higher quinolinic acid levels in CFAI OD_{600} 10 post-reaction versus the other groups (Supplemental Metabolomics Data). CFAI OD_{600} 10 also contained lower niacinamide concentrations than AI OD_{600} 10 (Supplemental Metabolomics Data). Pentose phosphate pathway metabolites' SUM_ribose-5-phosphate/ribulose-5-phosphate were in greater abundance in CFAI OD_{600} 10 than in AI OD_{600} 10 post-reaction (Figure 5). Lastly, lactate levels were lower in CFAI OD_{600} 10 post-reaction than AI OD_{600} 10 (Figure 5). These data highlight the metabolites uniquely associated with highly active extracts from high OD_{600} 10 harvests. These data suggest that the active metabolism within the extract may be equally important as the metabolic profile of the extract itself.

An additional focal point of this experiment was the differentiation of the metabolomic profile of 2x YTPG OD_{600} 2.5 versus 2x YTPG OD_{600} 10 in order to identify a metabolic basis for poor-quality extracts from cells grown to high ODs. In the cell extract samples, univariate analysis identified 20 metabolites that were significantly different between groups ($p<0.05$), including one that passed FDR (FDR<0.05) (Supplemental Metabolomics Data). 2x YTPG OD_{600} 10 extracts had lower concentrations of reduced glutathione and higher concentrations of oxidized glutathione than 2x YTPG OD_{600} 2.5 (Figure 4). 2x YTPG OD_{600} 10 extracts also had decreased levels of alpha-hydroxybutyrate and higher niacinamide levels. In the post-reaction samples, univariate analysis identified 9 metabolites that were significantly different between groups ($p<0.05$), with none passing FDR (FDR<0.05) (Supplemental Metabolomics Data). Of particular note, 2-hydroxyglutarate and citrate levels were in the lower 2x YTPG OD_{600} 10 versus 2x YTPG OD_{600} 2.5 (Supplemental Metabolomics Data). As previously mentioned, reduced 2-hydroxyglutarate may reflect a change in NADH + H+/NAD+ ratio and acidity while citrate is a vital component of the Krebs cycle and is used for NADPH regeneration.[27]

Focusing on differences between CFAI and AI OD_{600} 10 versus their respective OD_{600} 2.5 extracts, each had higher levels of xanthurenic acid, tryptophan, glucuronate, and carnitine in their OD_{600} 10 extracts and lower levels of creatine, alpha-glycerophosphate, and sorbitol (Supplemental Metabolomics Data). The AI media type had higher levels of 2-hydroxyglutarate and SUM fumarate+malate in its OD_{600} 10 extracts but CFAI were not different between its OD_{600} 2.5 and OD_{600} 10 extracts (Supplemental Metabolomics Data). CFAI had higher levels of niacinamide and SUM ribose-5-phosphate+ribulose-5-phosphate in its OD_{600} 10 extracts but the AI media type was not different between its OD_{600} 2.5 and OD_{600} 10 extracts (Supplemental Metabolomics Data). Interestingly, in these extracts, alpha-hydroxybutyrate were differentially altered, with CFAI OD_{600} 10 having higher and AI lower levels (Supplemental Metabolomics Data). In terms of reaction sample differences between CFAI and AI OD_{600} 10 versus their respective OD_{600} 2.5 extracts, each had lower levels of alpha-glycerophosphate in their OD_{600} 10 extracts (Supplemental Metabolomics Data). CFAI had lower 2-hydroxyglutarate and higher niacinamide and quinolinic acid levels in its OD_{600} 10 reactions but AI were not different between its OD_{600} 2.5 and OD_{600} 10 reaction samples (Supplemental Metabolomics Data). AI had higher levels of carnitine and SUM fumarate+malate in its OD_{600} 10 reactions but AI were not different between its OD_{600} 2.5 and OD_{600} 10 reaction samples (Supplemental Metabolomics Data). Reaction sample lactate levels were differentially altered, with AI OD_{600} 10 having higher and CFAI lower levels (Supplemental Metabolomics Data).

Discussion

The results presented here demonstrate the development of an improved upstream workflow for performing *E. coli* crude lysate-based cell-free protein synthesis. The development of the CFAI media formulation uniquely enabled us to gain insights to the energy metabolism associated with highly-

productive and poorly-performing cell extracts as well as extracts from cells harvested at mid-log to stationary phases of growth.

The CFAI workflow provides four key advantages over past CFPS workflows by 1) decreasing the overall time from a three day process to just under 24 hours, 2) decreasing the labor and oversight required from the researcher, 3) increasing the extract obtained by >400%, and 4) creating a long-lasting autoinduction media formula that obviates the need for IPTG induction and allows for next day harvesting. Directly inoculating a 1 L volume of media with a loopful of colonies obviates the seed culture and reduces the workflow by an entire day's time. Although standard microbiology growth procedures often rely on a single colony to limit genetic variability, our concerns were minimized since our streak plates were generated from an isogenic glycerol stock. Additionally, many biotechnology endeavors utilize the inoculation of multiple colonies into liquid cultures to support their biotechnology applications.[28,29] Importantly, the cell extracts produced from our growths have been shown to have reproducible robustness from batch-to-batch, reducing immediate concerns associated with the genetic variability arising from multiple colonies. For these reasons, we maintain that inoculating with multiple colonies from a fresh plate (in good condition with viable cells and stored at 4°C) of BL21Star™(DE3) that is generated from an isogenic glycerol stock is suitable for CFPS applications. Next, the rationale for using a seed culture is to expedite cell growth in large volumes; the seed culture allowed researchers to begin growth of a 1 L culture at an OD_{600} of 0.1 - 0.3 in order to reach OD_{600} of 2.5 in a timely manner. The capacity to obtain robust extracts from high density cell cultures that have autoinduced T7 RNAP expression obviates the need to monitor cell densities for induction of T7 RNAP between OD_{600} of 0.6 - 0.8 or for harvest at mid-log phase and therefore, eliminating the need for seed cultures.[5,6,8,9,11]

Following cell harvest, the time needed to wash the bacterial pellet is reduced to a third by using one washing step instead of three which displayed no drop in overall productivity of the cell extract (Supplemental Figure 1). Given that cell pellets are increasingly difficult to resuspend after each wash, the practical time and labor savings are likely greater than 3-fold. Moreover, the CFAI media still allows for a typical OD_{600} 2.5 harvest if large quantities of extract are not necessary, and it achieves this cell density at a faster growth rate than standard 2x YTPG media (Supplemental Figure 5). As a result, a researcher can inoculate a loopful of colonies in the morning and harvest at OD_{600} 2.5 seven hours later prior to going home for the day. In addition to the aforementioned advantages, researchers looking to maintain their current workflows may find CFAI superior to 2x YTPG for improved growth rates as another source of time reduction (Supplemental Figure 5). Lastly, our data showed that CFAI-based extracts are not limited by T7 RNAP and do not benefit from supplementation of purified enzyme which suggests that there is sufficient induction of the *lac* operon throughout the growth period (Supplemental Figure 6).

Metabolomics results indicated changes in energy metabolism related to niacin and its associated metabolites in CFAI OD_{600} 10 extract and post-reaction samples. In particular, the tryptophan conversion to NAD^+ and $NAPD^+$ pathway had several altered metabolites that were higher in both the CFAI OD_{600} 10 and AI OD_{600} 10 samples versus all other groups. However, we were particularly interested in metabolome changes observed uniquely in CFAI OD_{600} 10 in order to identify the basis for highly productive extracts obtained from stationary phase growths. Its elevated alpha-hydroxybutyrate levels in extract samples may suggest a high NADH + H+/NAD+ ratio. Interestingly, post-reaction samples' lower levels of 2-hydroxyglutarate and lactate suggest the NADH + H+/NAD+ ratio and acidity were decreased which may support maintenance of cell extract quality.[26,27] This potential change in conditions may reflect the active metabolism in the reaction. Also differentiating the CFAI OD_{600} 10 metabolome were alterations in the pentose phosphate pathway. While SUM_ribose-5-phosphate/ribulose-5-phosphate levels were different than all but AI OD_{600} 10 in extract samples, CFAI OD_{600} 10 was distinguished in

higher levels even in post-reaction samples. Therefore, a continued activation of the pentose phosphate pathway may also support the sustained effectiveness of CFAI OD_{600} 10 for producing robust cell extracts. In addition to its production of pentose sugars, this pathway produces NADPH, a reducing agent for antioxidants such as glutathione.[25,26]

The 2x YTPG OD_{600} 2.5 metabolome, corresponding to highly-productive cell extracts, was different from the 2x YTPG OD_{600} 10 metabolome, corresponding to poorly-performing cell extracts. Most notably, the 2x YTPG OD_{600} 10 extracts had lower concentrations of reduced glutathione and higher concentrations of oxidized glutathione. In summary, when placing these metabolomics results in a CFPS context, NAD-derived reducing equivalents may fuel oxidative phosphorylation for the production of ATP *in vitro.*[14] Produced during the upstream cellular catabolic processes, these reducing equivalents allow oxidative phosphorylation to proceed within inverted membrane vesicles present in the *E. coli* extracts. Sustained elevation of pentose phosphate metabolites in the reaction samples were unique to CFAI. With the increased presence of pentose phosphate and tryptophan conversion to niacin pathway metabolites in our robust extracts and the role that these pathways play in reducing equivalent turnover, out data suggests a relationship between these pathways and robust cell-free protein synthesis reactions. Additionally, our observations of changes in redox balance in highly-productive extracts is consistent with previous efforts to improve CFPS yields through genome engineering of *E. coli* strains.[16]

Metabolomics data support prior observations that the metabolism within CFPS systems is malleable[32] and that cell growth conditions can affect the metabolic pathways that are active cell extracts. It is plausible that supplementation of specific metabolite formulations informed by these data may further augment CFPS reactions, such efforts will likely have to be undertaken in conjunction with the modulation of the respective metabolic enzymes and pathways. Therefore, additional efforts will be needed to determine whether overexpression or augmentation of these metabolic pathways, in concert with metabolite supplementation could further improve CFPS yields.

In all, these efforts have resulted in the development of a new upstream workflow for the preparation of *E. coli* cell extracts in addition to new insights in the relationship between cell-free metabolism and cell-free protein synthesis. The CFAI media-based workflow provides researchers and educators[33] with an economical and reproducible strategy to generate large volumes of robust cell extracts capable of producing over 1 mg/mL of reporter protein. Notably, a researcher stocked with CFAI media and a streak plate can go from cells to CFPS within 24 hours in a 'set it and forget it' manner. We hope this innovation will transform the workflow for existing CFPS researchers and reduce the barrier to entry for new users.

Methods

Materials. All materials used in this manuscript have been previously described[6] with the exception of D-lactose (Alfa Aesar), glycerol (Sigma), and MILLEX-HV 0.22 µm Filter Unit (MILLIPORE, Carrigtwohil, Co. Cork, Ireland).

Cell Growth. All growths derived from *E. coli* BL21Star™(DE3) cells (generously provided by the Jewett Laboratory) are acquired from a glycerol stock and streaked onto a fresh LB agar plate and stored at 4°C. Streak plates in good condition with viable cells were used for inoculation.

2x YTPG Media Growth. A solution of 750 mL 2x YTP was prepared by dissolving 5.0 g sodium chloride, 16.0 g of tryptone, 10.0 g of yeast extract, 7.0 g of potassium phosphate dibasic, and 3.0 g of potassium phosphate monobasic into Nanopure™ water. The solution was adjusted to a pH of 7.2 using 5 M KOH.

250 mL glucose solution was created by combining 250 mL of Nanopure™ water with 18 g of D-glucose. The 2x YTP was transferred to a 2.5 L Tunair™ baffled flask and the glucose solution was transferred to an autoclavable glass bottle. Both solutions were autoclaved for 30 minutes at 121°C. A single colony of *E. coli* BL21Star™(DE3) was inoculated into a seed culture of 50 mL of sterile LB and grown overnight at 37°C and 200 rpm. The following day, a 2.5 L Tunair™ baffled flask containing 1 L of 2x YTPG was inoculated from the seed culture to reach an OD_{600} of 0.1. The culture was incubated at 37°C while shaking at 200 rpm until OD_{600} reached 0.6. The 1 L media was then induced with a final concentration of 1 mM of Isopropyl β-D-1-thiogalactopyranoside (IPTG). The culture was then harvested at an OD_{600} of 2.5.

AI Media Growth. The autoinduction media was prepared by adopting the recipe developed by Studier, F. W..[18] In brief, 5.0 g of sodium chloride, 20.0 g of tryptone, 5.0 g of yeast extract, 7.0 g of potassium phosphate dibasic, and 3.0 g of potassium phosphate monobasic were dissolved into 960 mL of Nanopure™ water. The pH was then adjusted to 7.2 using 5.0 M KOH and autoclaved in the Tunair™ baffled flask for 30 minutes at 121°C. A separate 40 mL of sugar solution was prepared by dissolving 6.0 mL of 100% glycerol, 2.0 g of D-lactose, and 0.5 g of D-glucose into 34.0 mL of Nanopure™ water. This sugar solution was sterilized using syringe filter sterilization. Following the same procedure for a seed culture, a single colony of E. coli BL21Star™(DE3) was inoculated into 50 mL of LB in a 125-mL Erlenmeyer flask and grown overnight at 37°C and 200 rpm. The next day, a 2.5 L Tunair™ baffled flask containing 1 L of AI media combined with its sugar solution was inoculated from the seed overnight culture to reach a starting OD_{600} of 0.1. The culture was harvested at an OD_{600} of 2.5.

CFAI Media Growth. CFAI media was prepared by dissolving 5.0 g of sodium chloride, 20.0 g of tryptone, 5.0 g of yeast extract, 14.0 g of potassium phosphate dibasic, and 6.0 g of potassium phosphate, monobasic into 960 mL of Nanopure™ water. Subsequently, the pH was adjusted to 7.2 using 5.0 M KOH and autoclaved for 30 minutes at 121°C. A separate sugar solution was prepared by dissolving 6.0 mL of glycerol, 4.0 g of D-lactose, and 0.5 g of D-glucose into 34.0 mL of Nanopure™ water. The sugar solution was filter-sterilized. The two solutions were mixed to complete the CFAI recipe prior to inoculation. When indicated, glycerol concentrations were titrated (Supplemental Figure 3). The same seed culture inoculation procedure as above was followed for a 2.5 OD_{600} harvest. For high density cultures with no human intervention, a loopful (Supplemental Figure 1) of the previously streaked *E. coli* BL21Star™(DE3) was directly inoculated into 1 L of CFAI media contained in a 2.5 L Tunair™ baffled flask and incubated at 30°C while shaking at 200 rpm. The culture was grown overnight (approximately 15 hours) to an approximate OD_{600} of 10. In some cases, specified amounts of supplemental glycerol were spiked into the culture after overnight growth, an hour prior to harvest.

Super CFAI Media Growth. Super-CFAI media consisted of 5.0 g of sodium chloride, 32.0 g of tryptone, 20.0 g of yeast extract, 14.0 g of potassium phosphate dibasic, and 6.0 g of potassium phosphate, monobasic into 960 mL of Nanopure™ water. After the pH was adjusted to 7.2 using 5.0 M KOH, the solution was transferred and autoclaved in a 2.5 L Tunair™ baffled flask and autoclaved for 30 minutes at 121°C. A separate sugar solution was prepared by dissolving 6.0 mL of glycerol, 4.0 g of D-lactose, and 0.5 g of D-glucose into 34.0 mL of Nanopure™ water. The sugar solution was syringe filter sterilized. These solutions were combined and inoculated with a loopful of colonies and grown overnight at 30°C shaking at 200 rpm.

Cell Harvest. The 1 L media was transferred into a cold 1 L centrifuge bottle (Beckman Coulter, Indianapolis, IN), then centrifuged at 5000 x g and 10°C for 10 minutes (Avanti® J-E Centrifuge, Beckman Coulter, Indianapolis, IN). After decanting the supernatant, the remaining pellet was transferred to a cold, tared, 50 mL Falcon tube using a sterile spatula (SmartSpatula®, LevGo, Inc., Berkeley, CA) while kept on ice. Then, cells were washed once with 40-50 mL of cold S30 buffer (14 mM $Mg(OAc)_2$, 10 mM Tris(OAc), 60 mM KOAc, 2 mM dithiothreitol) by resuspension via vortexing with rest periods on ice. In some specified cases, three washes were performed. The resuspension was centrifuged at 5000 x g and 10°C for 10 minutes. After disposing the supernatant, the pellet was weighed, then flash frozen via liquid nitrogen and kept at -80°C until extract preparation. When extracts were prepared during the same day as the harvest, each pellet was flash frozen prior to lysis.

Extract Preparation. The frozen cell pellet was combined with 1 mL of S30 buffer per 1 gram of cell pellet and thawed on ice. Once thawed, the cell pellet was resuspended via vortexing with rest periods on ice until no visible clumps of cells were observed. Then, 1.4 mL of the solution was transferred into 1.5mL Eppendorf tubes. A Q125 Sonicator (Qsonica, Newtown, CT) with a 3.175 mm probe was used at a frequency of 20 kHz and 50% amplitude with three forty-five seconds on/fifty-nine seconds off cycles to perform cell lysis. Immediately after, 4.5 µL of 1 M DTT was added to the lysate and inverted several times. The lysate was then centrifuged using a Microfuge 22R Tabletop Centrifuge (Beckman Coulter, Indianapolis, IN) at 18,000 × g and 4°C for 10 minutes. Following centrifugation, the supernatant was pipetted into a new 1.5 mL Eppendorf tube, flash frozen in liquid nitrogen, and kept in a -80°C freezer until use.

Cell-free Protein Synthesis. Cell-free protein synthesis was performed in 15 µL reactions in 1.5 mL Eppendorf tubes in triplicate unless otherwise noted. The standard condition of the reaction included 16 ng/µL of pJL1-sfGFP plasmid, 2.1 µL of Solution A (1.2 mM ATP, 0.850 mM GTP, 0.850 mM UTP, 0.850 mM CTP, 31.50 µg/mL folinic acid, 170.60 µg/mL tRNA, 0.40 mM nicotinamide adenine dinucleotide (NAD), 0.27 mM coenzyme A (CoA), 4.00 mM oxalic acid, 1.00 mM putrescine, 1.50 mM spermidine, and 57.33 mM HEPES buffer), 2.2 µL of Solution B (10 mM $Mg(Glu)_2$, 10 mM $NH_4(Glu)$, 130 mM K(Glu), 2 mM each of the 20 amino acids, and 0.03 M phosphoenolpyruvate (PEP)), 5.0 µL of cell extract, and a varying volume of molecular-grade water to fill the reaction volume to 15 µL [6]. Supplemental reactions included the exogenous addition of 100 µg/mL T7 RNAP (generously provided by the Jewett Laboratory). The cell-free protein synthesis reaction was carried out at 37°C for a minimum of four hours.

Quantification of Reporter Protein. Fluorescence intensity of superfolder GFP (sfGFP) was measured in triplicate per reaction with excitation and emission wavelengths of 485 and 528 nm respectively using a half area 96-well black polystyrene plate (Corning Incorporated, Corning, NY) containing 48 µL of 0.05 M HEPES solution (pH 7.2) and 2 µL of the cell-free protein synthesis reaction product. Fluorescence measurements were conducted using a Cytation 5 imaging reader (BioTek, Winwooski, VT). The fluorescence was then converted to concentration of sfGFP (µg/mL) based upon a standard curve as previously described.[6]

Metabolomics Analysis

Sample Preparation. Targeted metabolomics assays for primary metabolomics and aminomics were performed on both *E. coli* extract and CFPS reaction products using protein precipitation extraction with liquid chromatography tandem quadrupole mass spectrometry using modified previously published methods.[34] Briefly, 25 µL of extract was added to microfuge tubes before being spiked with 20 µL

isotopically-labeled surrogates followed by 750 µL chilled methanol. Samples were then vortexed 1 min prior to being centrifuged at 12,000 rpm for 10 min. The supernatant was transferred to 1.5 mL HPLC amber glass vials, dried by centrifugal vacuum evaporation, and reconstituted in 3:1 methanol:acetonitrile containing 100 nM of 1 cyclohexyl ureido, 3 dodecanoic acid (Sigma Aldrich). The reconstituted solution was vortexed 1 min and filtered at 0.1 µm by centrifugation at 9,500 rpm for 3 min through PVDF Durapore membranes (Millipore, Billerica, MA).

Mass Spectrometry. All UPLC-MS analyses were conducted on a Waters Acquity I-Class UPLC (Waters, Milford, MA) coupled with an API 4000 QTrap (Sciex, Framingham, MA) using multiple reaction monitoring quantified with AB Sciex MultiQuant version 3.0. For the primary metabolomics assay, metabolites were separated using a 150 X 2.0mm Luna NH2 column (Phenomenex, Torrance, CA) and detected by negative ion mode electrospray ionization.[34,35] For the aminomics assay, metabolites were separated using a 150 X 2.1mm Atlantis HILIC column (Waters) and detected by positive ion mode electrospray ionization.[34,36]

Statistical Analyses. Univariate statistical analyses were performed using one-way analysis of variance (ANOVA) on log transformed values. Tukey HSD posthoc tests were used to determine pairwise group differences. The significance levels (i.e. p-values) were assessed for multiple hypothesis testing according to Benjamini and Hochberg[37] at a false discovery rate (FDR) of 0.05. Interpretation of results is based on compounds with statistically significant raw p-values. All univariate analysis was performed using JMP Pro 14.0.0 (SAS Institute Inc.). Due to the low sample size resulting in a high propensity for overfitting when performing partial least squares-discriminant analysis (PLS-DA), we used the unsupervised method principal component analysis (PCA) for multivariate modeling using Metaboanalyst 3.0.[38]

ASSOCIATED CONTENT

Supplemental content includes a supplemental table describing media formulations, figures corresponding to cell growth curves under various growth media, CFPS reaction yields resulting from various modifications to the upstream processing steps, as well as metabolomics data.

AUTHOR INFORMATION

Corresponding Authors

* Michael La Frano: mlafrano@calpoly.edu

* Javin P. Oza: joza@calpoly.edu

Author Contributions

The manuscript was written through contributions of all authors, led by M.Z.L. All authors have given approval to the final version of the manuscript. M.Z.L, B.S., and A.C.M conducted the CFPS experiments; R.F., conducted metabolomics experiments; K.D. and M.L.F performed metabolomics data analysis; J.P.O conceived and led this work.

Funding Sources

Authors also acknowledge funding support from the Bill and Linda Frost Fund, Center for Applications in Biotechnology's Chevron Biotechnology Applied Research Endowment Grant, Cal Poly Research, Scholarly, and Creative Activities Grant Program (RSCA 2017), and the National Science Foundation (NSF-1708919). MZL would like to acknowledge the California State University Graduate Grant.

Notes

The authors declare no competing financial interest.

ACKNOWLEDGMENT

Authors would like to acknowledge Dr. Jennifer VanderKelen and Andrea Laubscher for technical support; Dr. Christopher Kitts, Dr. Michael Black, and Nicole Gregorio for helpful discussions.

ABBREVIATIONS

CFPS, cell-free protein synthesis; CFAI, cell-free autoinduction; sfGFP, superfolder green fluorescent protein; T7RNAP, T7 RNA polymerase; AI, autoinduction.

REFERENCES

(1) Gregorio, N. E., Levine, M. Z., and Oza, J. P. (2019) A User's Guide to Cell-Free Protein Synthesis. *Methods Protoc. 2*, 24.

(2) Carlson, E. D., Gan, R., Hodgman, C. E., and Jewett, M. C. (2012, September 1) Cell-free protein synthesis: Applications come of age. *Biotechnol. Adv.* Elsevier.

(3) Nirenberg, M. W., and Matthaei, J. H. (1961) The dependence of cell-free protein synthesis in E. coli upon naturally occurring or synthetic polyribonucleotides. *Proc. Natl. Acad. Sci.*

(4) Jewett, M. C., and Swartz, J. R. (2004) Mimicking the Escherichia coli cytoplasmic environment activates long-lived and efficient cell-free protein synthesis. *Biotechnol. Bioeng. 86*, 19–26.

(5) Kwon, Y. C., and Jewett, M. C. (2015) High-throughput preparation methods of crude extract for robust cell-free protein synthesis. *Sci. Rep. 5*, 8663.

(6) Levine, M. Z., Gregorio, N. E., Jewett, M. C., Watts, K. R., and Oza, J. P. (2019) Escherichia coli-Based Cell-Free Protein Synthesis: Protocols for a robust, flexible, and accessible platform technology. *J. Vis. Exp.*

(7) Dopp, J. L., and Reuel, N. F. (2018) Process optimization for scalable E. coli extract preparation for cell-free protein synthesis. *Biochem. Eng. J. 138*, 21–28.

(8) Shrestha, P., Holland, T. M., and Bundy, B. C. (2012) Streamlined extract preparation for Escherichia coli-based cell-free protein synthesis by sonication or bead vortex mixing. *Biotechniques 53*, 163–174.

(9) Sun, Z. Z., Hayes, C. A., Shin, J., Caschera, F., Murray, R. M., and Noireaux, V. (2013) Protocols for Implementing an Escherichia coli Based TX-TL Cell-Free Expression System for Synthetic Biology. *J. Vis. Exp.* e50762–e50762.

(10) Zawada, J. F., Yin, G., Steiner, A. R., Yang, J., Naresh, A., Roy, S. M., Gold, D. S., Heinsohn, H. G., and Murray, C. J. (2011) Microscale to manufacturing scale-up of cell-free cytokine production-a new approach for shortening protein production development timelines. *Biotechnol. Bioeng. 108*, 1570–1578.

(11) Liu, D. V., Zawada, J. F., and Swartz, J. R. (2005) Streamlining Escherichia Coli S30 extract preparation for economical cell-free protein synthesis. *Biotechnol. Prog. 21*, 460–465.

(12) Cole, S. D., Beabout, K., Turner, K. B., Smith, Z. K., Funk, V. L., Harbaugh, S. V., Liem, A. T., Roth, P. A.,

Geier, B. A., Emanuel, P. A., Walper, S. A., Chávez, J. L., and Lux, M. W. (2019) Quantification of Interlaboratory Cell-Free Protein Synthesis Variability. *ACS Synth. Biol. 8*, 2080–2091.

(13) Romantseva, E., and Strychalski, E. A. (2019) Cell-free workshop report. *Nist* 1–19.

(14) Jewett, M. C., Calhoun, K. A., Voloshin, A., Wuu, J. J., and Swartz, J. R. (2008) An integrated cell-free metabolic platform for protein production and synthetic biology. *Mol. Syst. Biol. 4*.

(15) Piir, K., Paier, A., Liiv, A., Tenson, T., and Maiväli, Ü. (2011) Ribosome degradation in growing bacteria. *EMBO Rep. 12*, 458–462.

(16) Martin, R. W., Des Soye, B. J., Kwon, Y. C., Kay, J., Davis, R. G., Thomas, P. M., Majewska, N. I., Chen, C. X., Marcum, R. D., Weiss, M. G., Stoddart, A. E., Amiram, M., Ranji Charna, A. K., Patel, J. R., Isaacs, F. J., Kelleher, N. L., Hong, S. H., and Jewett, M. C. (2018) Cell-free protein synthesis from genomically recoded bacteria enables multisite incorporation of noncanonical amino acids. *Nat. Commun. 9*, 1203.

(17) Hong, S. H., Kwon, Y. C., Martin, R. W., Des Soye, B. J., De Paz, A. M., Swonger, K. N., Ntai, I., Kelleher, N. L., and Jewett, M. C. (2015) Improving cell-free protein synthesis through genome engineering of Escherichia coli lacking release factor 1. *ChemBioChem 16*, 844–853.

(18) Studier, F. W. (2005) Protein production by auto-induction in high density shaking cultures. *Protein Expr. Purif. 41*, 207–234.

(19) Kim, R. G., and Choi, C. Y. (2000) Expression-independent consumption of substrates in cell-free expression system from Escherichia coli. *J. Biotechnol. 84*, 27–32.

(20) Kopp, J., Slouka, C., Ulonska, S., Kager, J., Fricke, J., Spadiut, O., and Herwig, C. (2017) Impact of Glycerol as Carbon Source onto Specific Sugar and Inducer Uptake Rates and Inclusion Body Productivity in E. coli BL21(DE3). *Bioengineering 5*, 1.

(21) Atlas, R. (2010) Handbook of Microbiological Media, Fourth Edition. *Handb. Microbiol. Media, Fourth Ed.*

(22) Gall, W. E., Beebe, K., Lawton, K. A., Adam, K. P., Mitchell, M. W., Nakhle, P. J., Ryals, J. A., Milburn, M. V., Nannipieri, M., Camastra, S., Natali, A., and Ferrannini, E. (2010) α-hydroxybutyrate is an early biomarker of insulin resistance and glucose intolerance in a nondiabetic population. *PLoS One 5*.

(23) Landaas, S., and Pettersen, J. E. (1975) Clinical conditions associated with urinary excretion of 2-hydroxybutyric acid. *Scand. J. Clin. Lab. Invest. 35*, 259–266.

(24) Mackay, D., Hathcock, J., and Guarneri, E. (2012) Niacin: Chemical forms, bioavailability, and health effects. *Nutr. Rev. 70*, 357–366.

(25) Kurnasov, O., Goral, V., Colabroy, K., Gerdes, S., Anantha, S., Osterman, A., and Begley, T. P. (2003) NAD Biosynthesis: Identification of the Tryptophan to Quinolinate Pathway in Bacteria. *Chem. Biol. 10*, 1195–1204.

(26) Intlekofer, A. M., Wang, B., Liu, H., Shah, H., Carmona-Fontaine, C., Rustenburg, A. S., Salah, S., Gunner, M. R., Chodera, J. D., Cross, J. R., and Thompson, C. B. (2017) L-2-Hydroxyglutarate production arises from noncanonical enzyme function at acidic pH. *Nat. Chem. Biol. 13*, 494–500.

(27) Oeggl, R., Neumann, T., Gätgens, J., Romano, D., Noack, S., and Rother, D. (2018) Citrate as Cost-

Efficient NADPH Regenerating Agent. *Front. Bioeng. Biotechnol. 6*.

(28) Pirman, N. L., Barber, K. W., Aerni, H. R., Ma, N. J., Haimovich, A. D., Rogulina, S., Isaacs, F. J., and Rinehart, J. (2015) A flexible codon in genomically recoded Escherichia coli permits programmable protein phosphorylation. *Nat. Commun. 6*.

(29) Zhu, P., Gafken, P. R., Mehl, R. A., and Cooley, R. B. (2019) A Highly Versatile Expression System for the Production of Multiply Phosphorylated Proteins. *ACS Chem. Biol. 14*, 1564–1572.

(30) Berg, J. M., Tymoczko, J. L., and Stryer, L. (2002) Glucose 6-Phosphate Dehydrogenase Plays a Key Role in Protection Against Reactive Oxygen Species, in *Biochemisty - 5th edition*, p Section 20.5 5-7.

(31) Stincone, A., Prigione, A., Cramer, T., Wamelink, M. M. C., Campbell, K., Cheung, E., Olin-Sandoval, V., Grüning, N. M., Krüger, A., Tauqeer Alam, M., Keller, M. A., Breitenbach, M., Brindle, K. M., Rabinowitz, J. D., and Ralser, M. (2015) The return of metabolism: Biochemistry and physiology of the pentose phosphate pathway. *Biol. Rev. 90*, 927–963.

(32) Caschera, F., and Noireaux, V. (2014) Synthesis of 2.3 mg/ml of protein with an all Escherichia coli cell-free transcription-translation system. *Biochimie 99*, 162–168.

(33) Williams, L. C., Gregorio, N. E., So, B., Kao, W. Y., Kiste, A. L., Patel, P. A., Watts, K. R., and Oza, J. P. (2020) The Genetic Code Kit: An open-source cell-free platform for biochemical and biotechnology education. *Front. Bioeng. Biotechnol. 8*, 941.

(34) Townsend, M. K., Clish, C. B., Kraft, P., Wu, C., Souza, A. L., Deik, A. A., Tworoger, S. S., and Wolpin, B. M. (2013) Reproducibility of metabolomic profiles among men and women in 2 large cohort studies. *Clin. Chem. 59*, 1657–1667.

(35) Bajad, S. U., Lu, W., Kimball, E. H., Yuan, J., Peterson, C., and Rabinowitz, J. D. (2006) Separation and quantitation of water soluble cellular metabolites by hydrophilic interaction chromatography-tandem mass spectrometry. *J. Chromatogr. A 1125*, 76–88.

(36) Wang, T. J., Larson, M. G., Vasan, R. S., Cheng, S., Rhee, E. P., McCabe, E., Lewis, G. D., Fox, C. S., Jacques, P. F., Fernandez, C., O'Donnell, C. J., Carr, S. A., Mootha, V. K., Florez, J. C., Souza, A., Melander, O., Clish, C. B., and Gerszten, R. E. (2011) Metabolite profiles and the risk of developing diabetes. *Nat. Med. 17*, 448–453.

(37) Benjamini, Y., and Hochberg, Y. (1995) Controlling the False Discovery Rate: A Practical and Powerful Approach to Multiple Testing. *J. R. Stat. Soc. Ser. B 57*, 289–300.

(38) Xia, J., and Wishart, D. S. (2016) Using metaboanalyst 3.0 for comprehensive metabolomics data analysis. *Curr. Protoc. Bioinforma. 2016*, 14.10.1-14.10.91.